JOC*Article*

Antioxidant Properties of Natural and Synthetic Chromanol Derivatives: Study by Fast Kinetics and Electron Spin Resonance Spectroscopy

Wolfgang Gregor,[†] Gottfried Grabner,[‡] Christian Adelwöhrer,[§] Thomas Rosenau,[§] and Lars Gille*[,†]

Research Institute for Pharmacology and Toxicology of Oxygen Radicals, University of Veterinary Medicine Vienna, Vienna, Austria, Max F. Perutz Laboratories, Department of Chemistry, University of Vienna, Vienna, Austria, and Department of Chemistry, University of Natural Resources and Applied Life Sciences, Vienna, Austria

Lars.Gille@vu-wien.ac.at

Received November 23, 2004

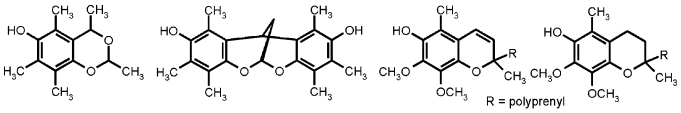

oxachromanol twin-chromanol ubichromenol ubichromanol

Chromanol-type compounds act as antioxidants in biological systems by reduction of oxygen-centered radicals. Their efficiency is determined by the reaction rate constants for the primary antioxidative reaction as well as for disproportionation and recycling reactions of the antioxidant-derived radicals. We studied the reaction kinetics of three novel chromanols: *cis*- and *trans*-oxachromanol and the dimeric twin-chromanol, as well as ubichromanol and ubichromenol, in comparison to α-tocopherol and pentamethylchromanol. The antioxidant-derived radicals were identified by optical and electron spin resonance spectroscopy (ESR). The kinetics of the primary antioxidative reaction and the disproportionation of the chromanoxyl radicals were assessed by stopped-flow photometry in different organic solvents to simulate the different polarities associated with biomembranes. Furthermore, the reduction of the chromanoxyl radicals by ubiquinol and ascorbate was measured after laser-induced one-electron chromanol oxidation in ethanol and in a micellar system, respectively. The rate constants showed that twin-chromanol had better radical scavenging properties than α-tocopherol and a significantly slower disproportionation rate of its corresponding chromanoxyl radical. In addition, the radical derived from twin-chromanol is reduced by ubiquinol and ascorbate at a faster rate than the tocopheroxyl radical. Finally, twin-chromanol can deliver twice as many reducing equivalents, which makes this compound a promising new candidate as artificial antioxidant in biological systems.

Introduction

The role of reactive oxygen species (ROS; e.g., peroxides, free oxygen-centered radicals) in the pathogenesis of many diseases has been recognized over the past decades.[1−3] This stimulated the exploration of counteracting strategies such as inhibition of ROS-forming enzymes (e.g., xanthine oxidase) or the control of pathophysiologically evolving radicals by chemical antioxidants on several levels of complexity, ranging from tests in mono- and biphasic chemical systems and subcellular or cellular model systems to tests on the organ and in whole organisms.[4] Vitamin E (α-tocopherol, **1**), ubiquitous in biomembranes, is believed to be the most important lipophilic antioxidant, inhibiting lipid peroxidation by a chain-breaking radical scavenging mechanism.[5−7] Even though its full repertoire of activities (which also includes nonantioxidant functions)[8] is far from being fully understood, the most complete pharmacological and toxicologi-

* Corresponding author: Research Institute for Pharmacology and Toxicology of Oxygen Radicals, University of Veterinary Medicine Vienna, Veterinärplatz 1, A-1210 Vienna, Austria; tel +43 1 25077 4407; fax +43 1 25077 4490; e-mail Lars.Gille@vu-wien.ac.at.

[†] University of Veterinary Medicine Vienna.

[‡] University of Vienna.

[§] University of Natural Resources and Applied Life Sciences.

(1) Sies, H. *Am. J. Med.* **1991**, *91S*, 31−38.

(2) Beal, M. F. *Ann. Neurol.* **1995**, *38*, 357−366.

(3) McCall, M. R.; Frei, B. *Free Radical Biol. Med.* **1999**, *26*, 1034−1053.

(4) Halliwell, B. *Free Radical Res. Commun.* **1990**, *9*, 1−32.

(5) Burton, G. W.; Ingold, K. U. *Ann. N.Y. Acad. Sci.* **1989**, *570*, 7−22.

(6) Brigelius-Flohe, R.; Traber, M. G. *FASEB J.* **1999**, *13*, 1145−1155.

(7) Pryor, W. A. *Free Radical Biol. Med.* **2000**, *28*, 141−164.

10.1021/jo047927s CCC: $30.25
Published on Web 03/30/2005

cal profile is available for this chromanol, among all natural and synthetic antioxidants.[5−7] Strategies to discover and design new antioxidants by derivatization of the evolutionarily favored chromanol structure used α-tocopherol as a starting structure, leading to new molecules such as Trolox.[9,10] Also the reported regulation of gene expression and enzyme activity by tocopherol[8] stimulated the development and study of new compounds in this class. While the medical application could profit from more active antioxidants overcoming transport limitations of natural antioxidant vitamins, the food and packaging industry is limited by the complicated technological properties of natural α-tocopherol and its uneconomic synthesis.

Unfortunately, in the past the quality of an antioxidant was often reduced to its radical scavenging activity. However, detailed studies on the oxidation products of vitamin E and ubiquinol have demonstrated that both antioxidant-derived radical intermediates (chromanoxyl and especially semiquinone radicals) and stable two-electron oxidation products (quinoid compounds) can compromise the overall benefit of an antioxidant.[11−14] Therefore, not only the bimolecular disproportionation of these radicals but also their recycling by hydrophilic or lipophilic cellular reductants must be considered. Since its discovery in 1979,[15] the reduction of the tocopheroxyl radical by ascorbate (vitamin C) has been widely covered in biochemical studies,[16,17] and evidence for its occurrence in vivo has been presented.[18,19] Later the reduction of this radical by ubiquinol (reduced coenzyme Q) has been documented as well.[20,21] Yet kinetic information on the reaction of these and related radicals is scarce. Furthermore, no single study so far has presented kinetic data for both the primary antioxidative reaction and the disproportionation and recycling reactions of the chromanoxyl radical, measured under comparable conditions, not even for vitamin E. Here we report a complete set of rate constants for these reactions to characterize novel synthetic antioxidants derived from the chromanol core of vitamin E (twin-chromanol and oxachromanols) and similar compounds synthesized from naturally occurring ubiquinone (ubichromanol and ubichromenol).

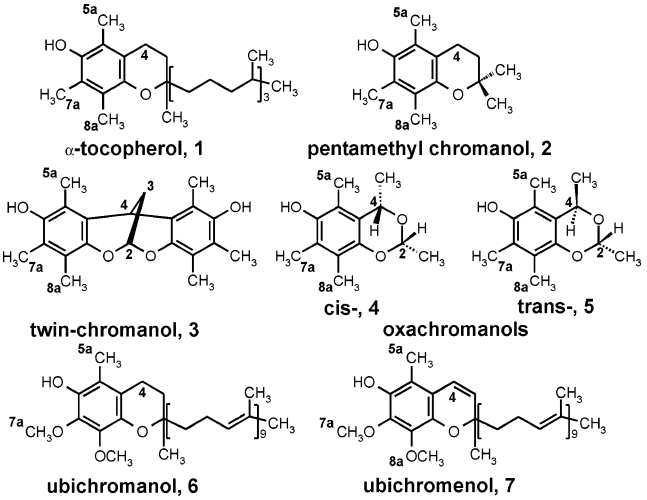

Twin-chromanol[22] and several oxachromanol derivatives including two dimethyl isomers[23,24] have recently been synthesized by Rosenau and co-workers to explore the redox properties of new chromanol structures. Ubichromenol was isolated from various animal tissues as well as synthesized from ubiquinone[25] and received some attention as a hypothetical intermediate in the overall process of oxidative phosphorylation. Whereas this idea was rejected, the reported antioxidant properties of this compound[26] seem more conceivable, although it is still unknown if ubichromenol is biosynthesized as a functional compound or if it is just a minor degradation ("waste") product. On the other hand, the related ubichromanol was never isolated from nature, but has also been synthesized from ubiquinone.[25]

The aim of this study was a comprehensive description of the antioxidant-related kinetic properties of the novel as well as ubiquinol-derived chromanols in comparison to vitamin E; to this end we investigated the influence of chromanol derivatization on the reactivities of both the parent chromanol and the chromanoxyl radical. Since in biological systems such antioxidants may function in environments with different physicochemical properties (e.g., the core of the lipid membranes or the polar headgroup region of phospholipids), we extended this kinetic investigation to various solvents, which were employed to mimic the environment in different membrane regions. On the basis of these results, the most promising antioxidant will be selected for future tests in biological systems.

Results

Compounds Studied. We studied the antioxidant properties of phenolic compounds (PhOH) that have recently been synthesized de novo — twin-chromanol (**3**)[22] and oxachromanols (**4**, **5**)[23,24] — or derived from natural ubiquinone (UQ-10) by chemical modification — ubichromanol (**6**) and ubichromenol (**7**). Dimeric chromanol structures and benzodioxines have not been

(8) Azzi, A.; Stocker, A. *Prog. Lipid Res.* **2000**, *39*, 231−255.
(9) Giulivi, C.; Romero, F. J.; Cadenas, E. *Arch. Biochem. Biophys.* **1992**, *299*, 302−312.
(10) Iuliano, L.; Pedersen, J. Z.; Camastra, C.; Bello, V.; Ceccarelli, S.; Violi, F. *Free Radical Biol. Med.* **1999**, *26*, 858−868.
(11) Siegel, D.; Bolton, E. M.; Burr, J. A.; Liebler, D. C.; Ross, D. *Mol. Pharmacol.* **1997**, *52*, 300−305.
(12) Gille, L.; Staniek, K.; Nohl, H. *Free Radical Biol. Med.* **2001**, *30*, 865−876.
(13) Moore, A. N.; Ingold, K. U. *Free Radical Biol. Med.* **1997**, *22*, 931−934.
(14) Nohl, H.; Gille, L.; Kozlov, A. V. *Free Radical Biol. Med.* **1998**, *25*, 666−675.
(15) Packer, J. E.; Slater, T. F.; Willson, R. L. *Nature* **1979**, *278*, 737−738.
(16) Bisby, R. H.; Parker, A. W. *FEBS Lett* **1991**, *1*, 205−208.
(17) Mukai, K.; Nishimura, M.; Kikuchi, S. *J. Biol. Chem.* **1991**, *266*, 274−278.
(18) Huang, J.; May, J. M. *Mol. Cell. Biochem.* **2003**, *247*, 171−176.
(19) Kagan, V. E.; Kuzmenko, A. I.; Shvedova, A. A.; Kisin, E. R.; Li, R.; Martin, I.; Quinn, P. J.; Tyurin, V. A.; Tyurina, Y. Y.; Yalowich, J. C. *Biochim. Biophys. Acta* **2003**, *1620*, 72−84.
(20) Kagan, V.; Serbinova, E.; Packer, L. *Biochem. Biophys. Res. Commun.* **1990**, *169*, 851−857.
(21) Mukai, K.; Kikuchi, S.; Urano, S. *Biochim. Biophys. Acta* **1990**, *1035*, 77−83.
(22) Rosenau, T.; Potthast, A.; Hofinger, A.; Kosma, P. *Angew. Chem., Int. Ed.* **2002**, *41*, 1171−1173.
(23) Rosenau, T.; Potthast, A.; Elder, T.; Lange, T.; Sixta, H.; Kosma, P. *J. Org. Chem.* **2002**, *67*, 3607−3614.
(24) Adelwöhrer, C.; Rosenau, T.; Gille, L.; Kosma, P. *Tetrahedron* **2003**, *59*, 2687−2691.
(25) Hatefi, Y. *Adv. Enzymol.* **1963**, *25*, 275−328.
(26) Burlakova, E. B.; Storozhok, M. M.; Khrapova, N. G. *Vopr. Pitan.* **1990**, *4*, 53−58.

studied as antioxidants so far, and for **6** and **7** detailed kinetic information is still missing.[27] For reference purposes, α-tocopherol (**1**) and pentamethylchromanol (**2**) were included in the study. The structures of **6** and **7** have been confirmed by ^{1}H and ^{13}C NMR. The peak assignments are in agreement with chemical shifts reported for ubichromanol-0,[28] ubichromenol-1,[27] ubichromenol-6,[29] and the polyprenyl chain of UQ-10.[30]

For transport processes in biological systems, the distribution of drugs between the aqueous phase and lipid membranes is of importance. Therefore, the lipophilicity of all compounds was assessed both by a theoretical approach and by experimental measurement of the octanol/water partition coefficients (*P*). The theoretical approach using the structure−activity relationship module of HyperChem[31] based on an incremental method of Ghose and co-workers[32,33] gave log *P* values of 9.6, 15.7, and 15.6 for the extremely lipophilic compounds **1**, **6**, and **7** (including the side chains), respectively. In contrast, experimental values for these compounds (**1**, ca. 6.2; **6** and **7**, ca. 5.2) were much smaller but still indicated a high lipophilicity. For short-chain compounds a better agreement of experimental and theoretical log *P* values was observed. Compounds **2**, **3**, **4**, and **5** gave theoretical values of 3.8, 5.7, 3.3, and 3.3, respectively. The corresponding experimental values were 3.7, 3.6, 3.2, and 3.2, respectively.

Identification of Radical Intermediates. It is known that lipophilic antioxidants exert their protective function in biological membranes by interception of reactive oxygen and nitrogen species. Since most of these species are radicals (R$^\bullet$), the antioxidant reaction can be characterized as a formal one-electron oxidation (eq 1) of the radical scavenging compounds including H-atom transfer and electron-transfer mechanisms.[34] Therefore, this reaction leads to the formation of an antioxidant radical (PhO$^\bullet$), which in turn can have a significant influence on the total benefit of an antioxidant.

$$\mathrm{PhOH} + \mathrm{R}^\bullet \rightarrow \mathrm{PhO}^\bullet + \mathrm{RH} \qquad (1)$$

To identify the phenoxyl radical intermediates, these were generated either by UV irradiation or by oxidation with the stable radical diphenyl picryl hydrazyl (DPPH$^\bullet$).[35,36] The ESR (electron spin resonance) spectra of the radicals are shown in Figure 1, clearly demonstrating the formation of paramagnetic one-electron oxidation products. Due to the highly resolved complex hyperfine structure, an intuitive guess of the coupling constants was difficult. Therefore, quantum chemical calculations were performed to predict the distribution of the unpaired electron and the coupling constants of the attached hydrogen atoms in the double-ring structure[37,38] (Table 1). Although these calculations do not take into account solvent effects, this starting approximation was useful to fit the experimental ESR spectra iteratively (Figure 1) and the quality of the simulations can be assessed from the comparison of an expanded section of the experimental spectra (insets of Figure 1, top traces) with the simulated spectra (bottom traces). The resulting coupling constants are also given in Table 1. The couplings are assigned according to our calculations (Table 1); for **1** and **2** they are in agreement with the literature.[28,39] The novel oxachromanol isomers exhibited coupling constants for the methyl protons similar to those in **1** and **2**. Interestingly, the coupling constants for the protons in the oxa ring (positions 2 and 4) were different for the cis (**4**) and trans derivatives (**5**). This assignment was confirmed by the simulation of ESR spectra from radicals of **4** and **5** deuterated in positions 2 and 4 (CD and CD_3), giving coupling constants for the respective

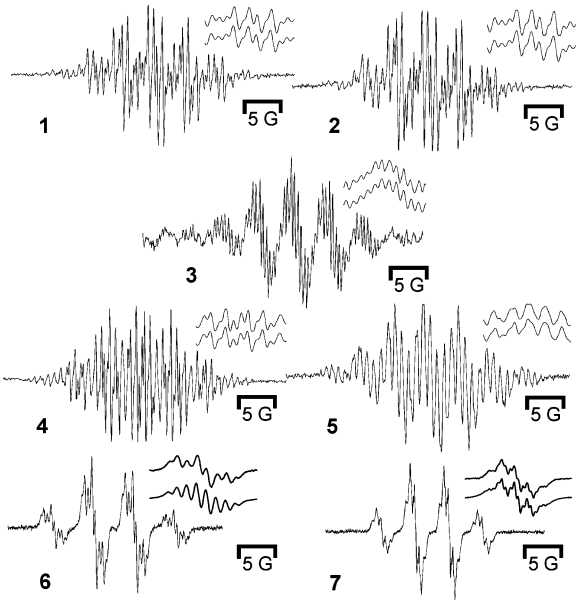

FIGURE 1. ESR spectra of phenoxyl radicals generated by UV irradiation of 50 mM solutions of **1**−**5** in benzene or by oxidation of 3 mM solutions of **6** and **7** in benzene with PbO_2, all under anaerobic conditions at room temperature. For each compound, the center multiplets of the experimental (top) and simulated spectra (bottom) are shown in the inset at an expanded field scale.

(27) Mukai, K.; Okabe, K.; Hosose, H. *J. Org. Chem.* **1989**, *54*, 557−560.
(28) Mukai, K.; Ikeuchi, T.; Morimoto, C.; Ishizu, K. *Tetrahedron Lett.* **1984**, *25*, 1929−1932.
(29) Imada, M.; Morimoto, H. *Chem. Pharm. Bull.* **1964**, *12*, 1047−1051.
(30) Boers, R. B.; Gast, P.; Hoff, A. J.; de Groot, H. J. M.; Lugtenburg, J. *Eur. J. Org. Chem.* **2002**, *1*, 189−202.
(31) Hyperchem [6.0]; HyperCube, Inc.: Gainesville, FL, 1994.
(32) Ghose, A. K.; Pritchett, A.; Crippen, G. M. *J. Comput. Chem.* **1988**, *9*, 80−90.
(33) Viswanadhan, V. N.; Ghose, A. K.; Revankar, G. R.; Robins, R. K. *J. Chem. Inf. Comput. Sci.* **1989**, *29*, 163−172.
(34) Foti, M.; Ruberto, G. *J. Agric. Food Chem.* **2001**, *49*, 342−348.
(35) Boguth, W.; Niemann, H. *Int. Z. Vitaminforsch.* **1969**, *39*, 429−437.
(36) Boguth, W.; Niemann, H. *Biochim. Biophys. Acta* **1971**, *248*, 121−130.
(37) Xie, C. P.; Lahti, P. M.; George, C. *Org. Lett.* **2000**, *2*, 3417−3420.
(38) Frisch, M. J.; Trucks, G. W.; Schlegel, H. B.; Scuseria, G. E.; Robb, M. A.; Cheeseman, J. R.; Zakrzewski, V. G.; Montgomery, J. A.; Stratman, R. E.; Burant, J. C.; Dapprich, S.; Millam, J. M.; Barone, V.; Cossi, M.; Cammi, R.; Mennucci, B.; Pomelli, C.; Adamo, C.; Clifford, S.; Ochterski, J.; Petersson, G. A.; Ayala, P. Y.; Cui, Q.; Morokuma, K.; Malick, D. K.; Rabuck, A. D.; Raghavachari, K.; Foresman, J. B.; Cioslowski, J.; Ortiz, J. V.; Stefanov, B. B.; Liu, G.; Liashenko, A.; Piskorz, P.; Komaromi, I.; Gomperts, R.; Martin, R. L.; Fox, D. J.; Keith, T.; Al-Laham, M. A.; Peng, C. Y.; Nananyakkara, A.; Gonzalez, C.; Challacombe, M.; Gill, P. M. W.; Johnson, B.; Chen, W.; Wong, M. W.; Andres, J. L.; Head-Gordon, M.; Replogle, E. S.; Pople, J. A. Gaussian 98 [revision A.6]; Gaussian Inc.: Pittsburgh, PA, 1998.
(39) Tsuchiya, J.; Niki, E.; Kamiya, Y. *Bull. Chem. Soc. Jpn.* **1983**, *56*, 229−232.

TABLE 1. Characterization of Phenoxyl Radicals by Quantum Chemical Calculations and by ESR and UV/Vis Spectroscopy

PhO•	a_0[a]/G (ab initio calculations)		a_0[a]/G (exptl)		λ_{max}/nm (ethanol)	ϵ[b]/L mol^{-1} cm^{-1} (ethanol)
1	3H(^{5a}CH$_3$)	6.49[c]	3H	6.02	426	3800 ± 800
	3H(^{7a}CH$_3$)	4.52[c]	3H	4.62		
	3H(^{8a}CH$_3$)	1.68[c]	3H	0.98		
	1H(^{4}CH$_2$)	2.79[c]	3H	1.58		
	1H(^{4}CH$_2$)	1.98[c]	1H	1.49		
2	3H(^{5a}CH$_3$)	6.49	3H	6.01	426	4800 ± 700
	3H(^{7a}CH$_3$)	4.52	3H	4.63		
	3H(^{8a}CH$_3$)	1.68	3H	0.98		
	1H(^{4}CH$_2$)	2.79	1H	1.56		
	1H(^{4}CH$_2$)	1.98	1H	1.55		
3	3H(^{5a}CH$_3$)	5.99	3H	5.60	415	2200 ± 200
	3H(^{7a}CH$_3$)	5.15	3H	5.45		
	3H(^{8a}CH$_3$)	1.87	3H	0.55		
	1H(^{4}CH)	0.71	1H	1.23		
	1H(^{3}CH$_2$)	0.38	1H	1.18		
	1H(^{2}CH)	0.22	1H	0.99		
	1H(^{3}CH$_2$)	0.02	1H	0.98		
4	3H(^{5a}CH$_3$)	6.13	3H	6.15	417	4000 ± 800
	3H(^{7a}CH$_3$)	5.40	3H	4.63		
	3H(^{8a}CH$_3$)	1.89	3H	1.03		
	1H(^{4}CH)	1.67	1H	2.38		
	1H(^{2}CH)	1.44	1H	1.48		
5	3H(^{5a}CH$_3$)	6.03	3H	6.32	421	2400 ± 100
	3H(^{7a}CH$_3$)	5.34	3H	4.83		
	3H(^{8a}CH$_3$)	1.86	3H	0.92		
	1H(^{4}CH)	1.84	1H	1.33		
	1H(^{2}CH)	0.01	1H	1.17		
6	3H(^{5a}CH$_3$)	4.75[c]	3H	5.72	425	3400 ± 200
	3H(^{7a}OCH$_3$)	2.04[c]	3H	0.45		
	1H(^{4}CH$_2$)	1.01[c]	3H	1.00		
	1H(^{4}CH$_2$)	0.69[c]	1H	1.00		
7	3H(^{5a}CH$_3$)	3.89[c]	3H	4.62	475	1000 ± 300
	3H(^{7a}OCH$_3$)	2.26[c]	3H	0.60		
	3H(^{8a}OCH$_3$)	0.06[c]	3H	0.17		
	1H(^{4}CH)	0.34[c]	1H	0.60		

[a] Isotropic hyperfine coupling constant. [b] Molar extinction coefficient; statistics are derived from sets of 3−10 measurements.[c] **2**, ubichromanol-1, and ubichromenol-1 were calculated instead of **1**, **6**, and **7**, respectively.

atoms about 6 times smaller than for the H-substituted compounds (not shown). Thus the coupling constants scale with the gyromagnetic ratios (H/D = 6.15) as expected.

To use optical detection methods for kinetic measurements, characterization of the radical absorption in the visible range was required. The chromanoxyl radical of **1** (tocopheroxyl) absorbs in the visible range, peaking at 425 nm.[35,40] The resulting spectra (Figure 2) of all radical intermediates obtained by oxidation of the phenolic compounds by UV irradiation, DPPH•, or PbO_2 are very similar, except that the ubichromenoxyl radical shows a significant red shift and broadening of its peak due to its extended conjugated π-system. For the other compounds the shifts are small (see also Table 1). For each compound the extinction coefficient in ethanol was estimated (Table 1). In acetonitrile, similar values (±15%) were obtained (not shown). The extinction coefficients of the radicals of **1** and **2** are in reasonable agreement with the values reported for similar chromanoxyl radicals in ethanol by Mukai et al.[40] (which are the only published values to date, except ca. 7000−8000 L mol^{-1} cm^{-1} in an apolar solvent),[35] demonstrating the reliability

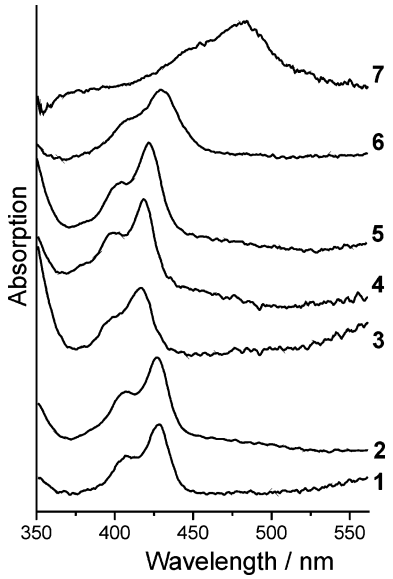

FIGURE 2. UV/Vis spectra of phenoxyl radicals generated by UV irradiation of 50 mM solutions of **1**−**5** or by reaction of 1 mM solutions of **6** and **7** with 20 μM DPPH•, in benzene (**6**) or acetonitrile (others) under aerobic conditions.

of our method. These data were used for further kinetic analysis.

Efficiency of the Phenolic Antioxidants. The reactivity of the phenolic compounds as antioxidants was tested by characterizing their reaction with the model radical DPPH• according to eq 2. In contrast to highly oxidizing radicals, fully substituted phenoxyl radicals (PhO•) only poorly react with DPPH• and do not interfere with the decay of this model radical.[41] Although DPPH• is a nitrogen-centered radical, it is known that its reaction rates with antioxidants give good approximations for the relative radical scavenging activities with lipid peroxyl radicals.[42,43] The decay of the DPPH• radical during the rapid reaction with the antioxidants was followed photometrically by the stopped-flow technique, as shown for **3** in Figure 3 (solid trace).

$$\text{DPPH}^\bullet + \text{PhOH} \xrightarrow{k_1} \text{DPPH-H} + \text{PhO}^\bullet \qquad (2)$$

The second-order rate constants (k_1) obtained for this reaction in three organic solvents are listed in Table 2. The large excess (10−35-fold) of antioxidant over DPPH• results in a stoichiometric factor of 1.0 since formally only one electron of each antioxidant molecule is contributing to the observed reaction. Control experiments under anaerobic conditions gave the same results as experiments with air-saturated solvents.

Fate of the Antioxidant-Derived Radical. The phenoxyl radical still possesses one reducing equivalent. However, as known for α-tocopherol, the chromanoxyl radicals are less effective as radical scavengers than the

(40) Mukai, K.; Watanabe, Y.; Ishizu, K. *Bull. Chem. Soc. Jpn.* **1986**, *59*, 2899−2900.
(41) Gille, L.; Prösch, U.; Stoesser, R. *Radiat. Phys. Chem.* **1992**, *40*, 461−468.
(42) Brand-Williams, W.; Cuvelier, M. E.; Berset, C. *Lebensm.-Wiss. Technol.* **1995**, *28*, 25−30.
(43) Foti, M. C.; Johnson, E. R.; Vinqvist, M. R.; Wright, J. S.; Barclay, L. R.; Ingold, K. U. *J. Org. Chem.* **2002**, *67*, 5190−5196.

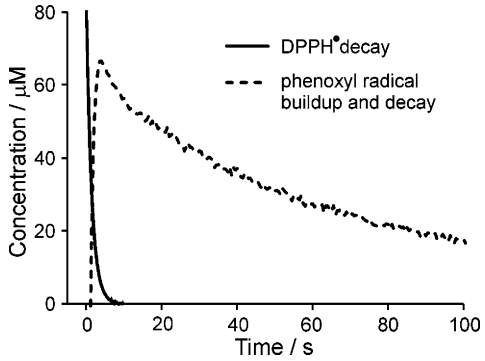

FIGURE 3. Kinetic traces obtained by stopped-flow photometry for the reaction of 8 mM **3** with 200 μM DPPH• in aerobic ethanol at 20 °C.

TABLE 2. Second-Order Rate Constants Obtained from Stopped-Flow Measurements at 20 °C for the Reaction of DPPH• with Phenolic Antioxidants in Homogenous Solutions of Different Solvents

	k_1/L mol^{-1} s^{-1}		
PhOH	AcN[a,b]	ethanol[c]	hexane[c]
1	350 ± 7	245 ± 15	6850 ± 150
2	325 ± 25	253 ± 9	6750 ± 250
3	280 ± 19	376 ± 7	50 100 ± 2100[d]
4	52 ± 2	107 ± 5	2250 ± 250
5	39 ± 2	73 ± 13	1770 ± 50
6	92 ± 31	122 ± 15	450 ± 90
7	54 ± 12	136 ± 53	370 ± 40

[a] Acetonitrile. [b] Statistics are derived from sets of 3−7 measurements. [c] Statistics are derived from sets of 2−4 measurements. [d] Statistics are derived from a set of 20 measurements.

corresponding chromanol.[44] Therefore, its reduction to the antioxidatively more active form (the phenol) is of major importance. Two principal pathways have been identified for this reduction: (1) the disproportionation ("self-decay") of two phenoxyl molecules to one molecule of phenol and one molecule of a quinoid oxidation product (tocopheryl quinone in the case of **1**) in a multistep reaction[45] and (2) the reduction of the phenoxyl radical by cellular reductants, such as ascorbate and ubiquinol (antioxidant recycling). Therefore, model experiments were performed to measure the rate constants for both pathways.

Disproportionation. The formation of phenoxyl radicals by oxidation of the phenols with DPPH• or PbO_2 and the decay of these radicals due to their disproportionation (eq 3) was followed at their respective absorption maxima (Figure 2 and Table 1), as shown for **3** in Figure 3 (dotted trace).

$$2\ \mathrm{PhO}^{\bullet} \xrightarrow{k_2} \mathrm{PhOH} + \mathrm{PhQ} \qquad (3)$$

Rate constants ($2k_2$) obtained from stopped-flow measurements in three organic solvents are shown in Table 3. The decay of all radicals studied was independent of the presence or absence of O_2 in the solutions. This poor reactivity with O_2 is well-known for radicals derived from highly substituted ("hindered") phenolic antioxidants[46]

TABLE 3. Second-Order Rate Constants Obtained from Optical Stopped-Flow and ESR Measurements at 20 °C for Disproportionation of Phenoxyl Radicals in Homogeneous Solutions of Different Solvents, Generated with DPPH• or PbO_2[a]

	$2k_2$/L mol^{-1} s^{-1}				
PhO•	DPPH•, optical, acetonitrile[b]	DPPH•, optical, ethanol[b]	DPPH•, optical, hexane[c]	DPPH•, ESR, acetonitrile[c]	PbO_2, optical, acetonitrile[c]
1	1890 ± 50	1060 ± 80	3120 ± 540	1170 ± 70	1730 ± 140
2	1610 ± 30	1070 ± 80	3310 ± 230	1020 ± 60	2340 ± 80
3	243 ± 21	267 ± 11	nd[d]	275 ± 38	820 ± 40
4	3560 ± 80	5240 ± 220	2070 ± 100	2100 ± 120	3770 ± 100
5	452 ± 41	614 ± 6	207 ± 25	630 ± 85	430 ± 30
6	1830 ± 360	1570 ± 220	1500 ± 90	650 ± 90	1260 ± 40
7	16.4 ± 0.7	57 ± 6	31 ± 9	19 ± 3	67 ± 1

[a] Column headings list method of generation, method of detection, and solvent. [b] Statistics are derived from sets of 3−5 measurements. [c] Statistics are derived from sets of 2−4 measurements. [d] Phenoxyl peak not detected.

and is a prerequisite for their successful function as biological antioxidants. Decay traces after generation of all phenoxyl radicals with an independent method (PbO_2 oxidation) revealed rate constants (Table 3) within the same range compared to those measured by stopped-flow photometry.

Recycling by Cellular Reductants. For antioxidant recycling studies we chose a hydrophilic (ascorbate) and a lipophilic reductant (ubiquinol), which have both been shown to reduce the tocopheroxyl radical.[15,17,20,21,47]

1. Recycling by Ascorbate. The active ascorbate species in biological systems has been reported to be its deprotonated anionic form (Asc^-),[17] which predominates at the pH (6.8) chosen in our experiments ($pK_1 = 4.2$, $pK_2 = 11.6$).[17] Since Asc^- is water-soluble, we have chosen a biphasic model system consisting of an aqueous buffer containing ascorbate and a lipophilic phase formed by TTAB micelles harboring the lipophilic antioxidants:

$$\mathrm{PhO}^{\bullet}_{\mathrm{micelle}} + \mathrm{Asc}^{-}_{\mathrm{aqueous\ phase}} + \mathrm{H}^{+} \xrightarrow{k_3} \mathrm{PhOH}_{\mathrm{micelle}} + \mathrm{Asc}^{\bullet}_{\mathrm{aqueous\ phase}} \qquad (4)$$

Preliminary experiments revealed that the reaction with DPPH• was too slow to generate measurable amounts of phenoxyl radicals in micelles. Since UV laser-induced monophotonic H-abstraction to generate phenoxyl radicals has been used by other groups,[16] we employed a laser emitting at 266 nm to generate the chromanoxyl radicals by flash photolysis. Following the laser pulse, the radical decay was detected photometrically. At this excitation wavelength the extinction coefficients of the studied chromanols are ca. 10−20% of their maximal absorptivity at 290 nm. For each phenolic compound the absorption maximum of the phenoxyl radical in micelles was determined in the absence of ascorbate by probing the visible spectrum in 5 nm steps. The absorption maxima observed (not shown) agree well (±5 nm) with the absorption maxima detected with the diode-array photometer (vide supra), except for **7**, which produced a nonreducible species with a considerably broader spectrum than

(44) Liebler, D. C.; Burr, J. A. *Biochemistry* **1992**, *31*, 8278−8284.
(45) Bowry, V. W.; Ingold, K. U. *J. Org. Chem.* **1995**, *60*, 5456−5467.
(46) Doba, T.; Burton, G. W.; Ingold, K. U.; Matsuo, M. *J. Chem. Soc., Chem. Commun.* **1984**, 461−462.
(47) Bisby, R. H.; Parker, A. W. *Arch. Biochem. Biophys.* **1995**, *317*, 170−178.

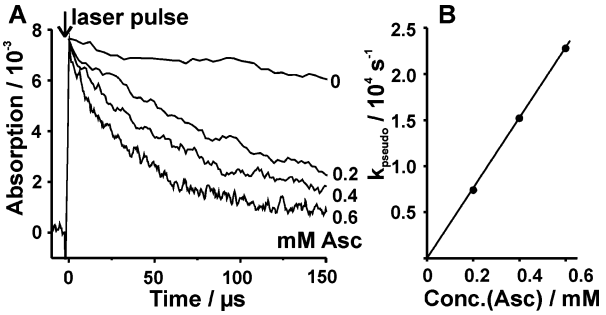

FIGURE 4. (A) Kinetic traces of the transient absorption of the radicals generated by laser flash photolysis of 1 mM **3**, incorporated into 40 mM aqueous TTAB micelles, in the absence and presence of ascorbate (Asc) at room temperature. (B) Plot of the measured pseudo-first-order rate constant k_{pseudo} (from which k_3 was derived) versus ascorbate concentration.

TABLE 4. Second-Order Rate Constants Obtained from Laser Flash Photolysis at 20 °C for the Reduction of Phenoxyl Radicals by Ascorbate (k_3) and Decylubiquinol (k_4)

PhO•	k_3[a]/10^7 L mol^{-1} s^{-1} (micelles)	k_4[a]/10^4 L mol^{-1} s^{-1} (ethanol)
1	1.1 ± 0.2	0.64 ± 0.14
2	2.6 ± 0.1	1.96 ± 0.21
3	3.7 ± 0.1	3.4 ± 2.0
4	4.2 ± 0.2	12.6 ± 1.4
5	10.4 ± 0.4	17.4 ± 1.5
6	0.90 ± 0.07	<1500 ± 500[b]
7	>0.003 ± 0.001[c]	>3 ± 1[c]

[a] Statistics are derived from sets of 5−9 measurements. [b] The second-order decay of the radical in the absence of quinol was too fast to resolve the quinol reaction, but control experiments showed the reducibility of the radical (see Results). [c] The expected radical species could not be generated photochemically; lower limits of the rate constants were estimated from experiments with PbO_2 -generated radicals.

expected. Similar effects were observed upon continuous UV irradiation of **7**. We assume that the chromenol ring structure is opened to a polyunsaturated isomer. Such a photochromic effect has been described for chromenes.[48] Due to the short pulse length of 10 ns, the phenoxyl radicals were generated much faster than their consumption by the reaction with ascorbate. Ascorbate concentrations were limited to a range that does not significantly influence the absorption of chromanols at 266 nm. Control experiments with ascorbate solutions, omitting the antioxidants, revealed no transient absorptions in the range of 410−480 nm, which was used for the detection of phenoxyl radicals. The resulting kinetic traces showed increasing decay rates with increasing concentrations of ascorbate, as shown for **3** in Figure 4A. The linear relationship between the observed pseudo-first-order rate constant (k_{pseudo}) and the ascorbate concentration (Figure 4B) confirms the bimolecular reduction of the radicals by ascorbate. The rate constants (k_3) obtained for the phenoxyl reduction are shown in Table 4. For **7**, only a lower limit could be estimated from conventional mixing of PbO_2-generated chromenoxyl with ascorbate (see Experimental Section). This limit corresponds to the kinetics of the mixing process itself, as evident from a control experiment in which a dye (DPPH•) was mixed with pure solvent (acetonitrile) and monitored at 520 nm (not shown).

2. Recycling by Ubiquinol. Using the same technique, we studied the reduction of photochemically generated phenoxyl radicals by decylubiquinol, an analogue of natural ubiquinol, in ethanolic solution (eq 8). Due to the similar absorption spectra of chromanols and ubiquinol around 266 nm and thus interference of the cogenerated ubisemiquinone radical, a direct photolytic generation of phenoxyl radicals turned out to be inappropriate. Therefore the phenoxyl radicals were generated indirectly by photolytic cleavage of the azo initiator 2,2′-azobis(2,4-dimethylvaleronitrile) (AMVN, R−N=N−R) at 355 nm according to eqs 5−7:

$$\mathrm{R{-}N{=}N{-}R} \xrightarrow{h\nu} 2\mathrm{R^\bullet} + \mathrm{N_2} \quad (5)$$

$$\mathrm{R^\bullet} + \mathrm{O_2} \rightarrow \mathrm{ROO^\bullet} \quad (6)$$

$$\mathrm{PhOH} + \mathrm{ROO^\bullet} \rightarrow \mathrm{PhO^\bullet} + \mathrm{ROOH} \quad (7)$$

Reaction of PhOH with rapidly formed ROO• is the major source of PhO•. At this wavelength the extinction coefficient of AMVN is ca. 90% of its peak absorption at 348 nm. A chromanol:ubiquinol concentration ratio of at least 10:1 favored the reaction of the initiator radicals with the chromanol (assuming a similar reactivity based on literature data of α-tocopherol and ubiquinol).[49] Control experiments with only azo initiator and ubiquinol (concentrations as used for kinetic experiments) did not yield significant absorptions in the 400−500 nm range. Although neutral ubisemiquinones have also been reported to show absorptions in this spectral range,[50] their disproportionation (eq 9) is so rapid ($k \approx 4 \times 10^7$ L mol^{-1} s^{-1})[51] that they do not interfere with the phenoxyl decay kinetics. The rate constants (k_4) obtained for the reduction of PhO• by decylubiquinol (eq 8) are shown in Table 4. For **6**, the second-order decay of the radical was too fast to resolve the quinol reaction; from this only an upper limit can be given. However, with a diode-array photometer the spectra from radicals of **6**, generated with PbO_2 in ethanol, disappeared within 30 s after admixing of 100 μM decylubiquinol (but not in the absence of reductant; not shown). For **7**, only a lower limit can be estimated as for the ascorbate reaction (vide supra).

$$\mathrm{PhO^\bullet} + \mathrm{UQH_2} \xrightarrow{k_4} \mathrm{PhOH} + \mathrm{UQH^\bullet} \quad (8)$$

$$\mathrm{UQH^\bullet} + \mathrm{UQH^\bullet} \rightarrow \mathrm{UQ} + \mathrm{UQH_2} \quad (9)$$

Number of Reducing Equivalents. Besides kinetic aspects of antioxidant efficiency, the total amount of reduction equivalents per molecule is of interest. We approached this question experimentally by completely oxidizing the phenolic compounds with an excess of DPPH• in acetonitrile. This integrates the number of

(48) Becker, R. S.; Michl, J. *J. Am. Chem. Soc.* **1966**, *88*, 5931−5933.

(49) Shi, H.; Noguchi, N.; Niki, E. *Free Radical Biol. Med.* **1999**, *27*, 334−346.

(50) Land, E. J.; Swallow, A. J. *J. Biol. Chem.* **1970**, *245*, 1890−1849.

(51) Roginsky, V. A.; Pisarenko, L. M.; Bors, W.; Michel, C. *J. Chem. Soc., Perkin Trans. 2* **1999**, *4*, 871−876.

reducing equivalents over the primary reaction and subsequent reactions, such as delivery of additional reducing equivalents via disproportionation of phenoxyl radicals. The presence of multiple OH groups in polyphenols such as flavonoids was often considered as evidence for higher antioxidative activity, which is not necessarily true.[52]

The DPPH• decay we obtained (not shown), until completion of the reaction, took about the same time as the decay of the phenoxyl radicals (as measured in our disproportionation experiment), as expected. Surprisingly we observed that for **3** and for the oxachromanol isomers the total number of reducing equivalents per molecule was related to the water content in the solvent. In dry solvent, **1**, **2**, **4**, **5**, **6**, and **7** delivered 2.0 ± 0.1, 1.9 ± 0.1, 2.0 ± 0.1, 2.1 ± 0.1, 2.0 ± 0.1, and 2.0 ± 0.1 equiv, respectively, as expected for a chromanol. In solvent containing 10% water the number was raised to 2.4 ± 0.1 for both oxachromanol isomers but not for **1**, **2**, **6**, and **7**. This suggested that an oxidation product was formed which can act as an antioxidant itself. Indeed Rosenau et al.[23] showed that oxachromanol undergoes water-dependent oxidative heterocycle opening to yield a hydroxyethylquinone, which isomerizes to a quinol form. Compound **3** delivered 2.8 ± 0.1 equiv in dry solvent and 4.1 ± 0.1 equiv in the presence of 10% water. Above 10% water, no further increase was observed for all compounds. The numbers obtained in aqueous solvent are certainly more relevant to biological systems.

Discussion

Distribution of Chromanol Antioxidants. All compounds studied are highly lipophilic (log *P* ca. 3−6), and therefore, they are expected to partition strongly into biomembranes. Thus they should be able to protect biological membranes from lipid peroxidation, although short- (**3**, **4**, and **5**) and long-chain compounds (**6** and **7**) may function in different regions of the membrane. Short- and long-chain tocopherol derivatives have been shown to exert similar antioxidative activities. However, their faster diffusional exchange rates between micelles and biomembranes could be a significant advantage of short-chain antioxidants with respect to pharmacological targeting.

Structure of Phenoxyl Radicals. To characterize the reactivities of the different phenoxyl radicals, we first identified them by ESR (Figure 1) and UV/Vis spectroscopy (Figure 2). ESR revealed the proton hyperfine coupling constants (Table 1), which reflect the electronic structure of the radicals, that is, the degree of electron delocalization, which influences radical stability and also antioxidant reactivity, because radical stability supports H-abstraction.[53] The proton coupling constants obtained for **1** and **2** are very similar to the ones reported.[39] The values obtained for the ubiquinone derivatives are similar to those reported for short-chain analogues.[28] Also, the reasonable agreement between experimental and theoretical coupling constants confirms the classification of all radicals as chromanoxyl or chromenoxyl radicals, taking into account that the quantum chemical calculations performed do not consider solvent effects. Furthermore, ESR data and quantum chemical calculations clearly demonstrate that the unpaired electron is not only located in the conjugated π-ring system but also extends to the oxa ring. In detail, the major coupling constants of the radical of **3** were significantly different from those of **1** and **2**, showing a more uniform distribution of the unpaired electron over positions 5 and 7 as well as more contribution from coupling hydrogens of the heterocyclic bridge, suggesting a higher degree of electron delocalization and hence a more stable radical. The smaller methyl coupling in **7** (4.6 G versus 5.7 G in **6**) indicates a higher degree of electron delocalization into the unsaturated heterocycle, again predicting a more stable radical. These findings suggest that chemical modifications of the oxa ring should modulate both the antioxidant activity and the radical stability, and possibly also the reactivity toward cellular reductants.

Primary Antioxidant Reaction. The use of DPPH• as a model radical represents a convenient method to evaluate the radical scavenging properties of antioxidative molecules and antioxidant plant extracts.[42] Since DPPH• and peroxyl radicals have similar electronic structures (the unpaired electron is delocalized over both N atoms of hydrazyl and both O atoms of peroxyl),[54] relative reactivities of antioxidants with DPPH• generally show the same order as with the more relevant lipid peroxyl radicals.[42,43] In our study we considered the variation of k_1 in dependence on both the antioxidant structure and the solvent in order to mimic different polarities in biomembranes (Table 2).

For the different structures we found a high-activity group (**1**−**3**) and a low-activity group (**4**−**7**) in ethanol and acetonitrile, while the two oxachromanol isomers (**4** and **5**) showed more intermediate activities in hexane. The k_1 values for **1** and **2** in hexane are almost identical with the ones measured in hydrocarbons,[55,56] whereas our value for **1** in acetonitrile is somewhat smaller than the one (490 L mol^{-1} s^{-1}) reported for this solvent.[55] Compound **3** reacts with the model radical approximately as fast as **1** and **2** in acetonitrile and ethanol or even 7 times faster in hexane. This cannot be accounted for by a statistical factor of 2, which would be expected for a dimeric chromanol in which the two OH groups act independently of each other as confirmed for a substituted bisphenol.[57] Therefore the higher reactivity of **3** must originate from its special electronic properties, in agreement with the larger stability of its radical (vide infra). In contrast, **4** and **5** react ca. 3−16 times more slowly than methyl-substituted compounds with only one O atom in the attached ring (**1**−**3**). While Mukai et al.[27] reported a 10 times lower reactivity of short-chain ubichromanol and ubichromenol analogues with a stable substituted phenoxyl radical in ethanol, in our experiments the rates of **6** and **7** were as high as 50% that of **1** in the same solvent. Therefore a biological antioxidant

(52) Metodiewa, D.; Jaiswal, A. K.; Cenas, N.; Dickancaite, E.; Segura-Aguilar, J. *Free Radical Biol. Med.* **1999**, *26*, 107−116.
(53) Burton, G. W.; Doba, T.; Gabe, E. J.; Hughes, L.; Lee, F. L.; Prasad, L.; Ingold, K. U. *J. Am. Chem. Soc.* **1985**, *107*, 7053−7065.
(54) Lucarini, M.; Pedulli, G. F.; Valgimigli, L. *J. Org. Chem.* **1998**, *63*, 4497−4499.
(55) Valgimigli, L.; Banks, J. T.; Ingold, K. U.; Lusztyk, J. *J. Am. Chem. Soc.* **1995**, *117*, 9966−9971.
(56) Barclay, L. R. C.; Edwards, C. E.; Vinqvist, M. R. *J. Am. Chem. Soc.* **1999**, *121*, 6226−6231.
(57) Amorati, R.; Lucarini, M.; Mugnaini, V.; Pedulli, G. F. *J. Org. Chem.* **2003**, *68*, 5198−5204.

function of the naturally occurring **7**[26] seems possible. The lower activity of the ubiquinone derivatives can be explained by intramolecular H-bonding between the phenolic OH group and the neighboring methoxy group,[58] similar to the intermolecular solvent effects outlined below. In contrast to the larger stability of the radical of **7** with respect to **6** (vide infra) which should enhance the antioxidant activity of **7**, we find comparable or even slightly smaller rates for **7**. Pentamethylchromenol also showed only 66% activity toward peroxyl radicals in an apolar solvent compared to its saturated analogue **2**.[53]

While the antioxidant reaction between phenols (PhOH) and radicals (R•) can proceed via H-atom transfer in apolar media (eq 10), in polar solvents the electron-transfer mechanism (eq 11) is more likely, and the rates are modulated by interference of the solvent, by inhibiting the formation of the intermediate complex or by accelerating the electron transfer within the caged complex between PhOH and R• (DPPH• in our experiments).[34]

$$R^{\bullet} + PhOH \rightarrow (R^{\bullet}\cdots H\cdots OPh)_{cage} \rightarrow R{-}H + PhO^{\bullet} \quad (10)$$

$$R^{\bullet} + PhOH \rightarrow (R^{-}\cdots {}^{+\bullet}HOPh)_{cage} \rightarrow R{-}H + PhO^{\bullet} \quad (11)$$

Since the rate constants k_1 (Table 2) for all compounds are considerably smaller in polar solvents (acetonitrile and ethanol) than in hexane, obviously hindrance of complex formation by H-bonding between solvent and the phenolic hydroxyl group seems to prevail, as has been found for tocopherol.[55,58] That the relative solvent effects can be quite different for different antioxidants, as seen in Table 2, has already been found for other compounds and has been explained by differential H-donor/acceptor interactions with the solvent.[56] Interestingly, **6** and **7** show the smallest solvent effect, suggesting that the intramolecular H-bond between the methoxy and OH groups is either retained in the more polar solvents or replaced by an H-bond of comparable strength. Several studies placed the prenyl chain of **1** parallel to the membrane lipid chains and the phenolic OH group H-bonding to the lipid carbonyl or phosphate groups.[59] The short-chain chromanols of the present study should insert into membranes even closer to the membrane–water interface. Therefore the kinetic properties obtained in H-bond donor (ethanol) or acceptor solvents (acetonitrile) are more relevant to the antioxidant performance in biomembranes than those obtained in hexane.

Studies of Hasford and Rizzo[60] and Caffery et al.[61] have demonstrated that the reduction potential of flavin model compounds is correlated with the energy of their lowest unoccupied molecular orbitals (LUMOs). Vice versa, the oxidation of chromanols should depend on the energy of their highest occupied molecular orbitals (HOMOs),

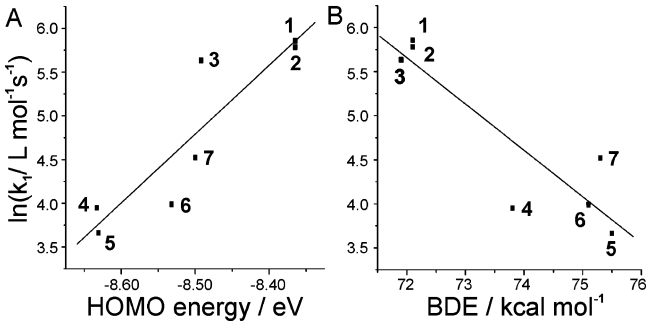

FIGURE 5. Correlation between the logarithm of the rate constants (ln k_1) of the antioxidant reaction with DPPH• in acetonitrile (Table 2) and the energy levels of the highest occupied molecular orbital (HOMO; panel A) or the O–H bond dissociation enthalpies (BDE) of the antioxidant (panel B).

especially if they transfer an electron in the antioxidative mechanism. HOMO energies as well as O–H bond dissociation enthalpies (BDE) of the chromanols were calculated by the semiempirical quantum chemical method PM3. By plotting the logarithm of the rate constants k_1 (in acetonitrile) versus the HOMO energies and BDE, the correlations shown in Figure 5 were obtained. The figure shows a fairly linear increase of reaction rates with increasing HOMO energies (panel A) and decreasing O–H bond dissociation enthalpies (panel B), confirming the thermodynamic control of this reaction in polar solvents. For the disproportionation (k_2) and recycling reactions (k_3, k_4) no correlation with the frontier orbital energies or BDE was found, suggesting that steric factors control these rates.

Fate of Antioxidant-Derived Radicals. Although several studies in the past dealt with the radical scavenging properties of chromanols,[27,53,55,56] none of these studies considered primary radical reaction, disproportionation, and radical recycling together. This is a major problem when different investigators use different solvents, since rate constants may differ by several orders of magnitude, as demonstrated by Table 2, thereby preventing adequate comparison of antioxidants with reference compounds, such as **1** and **2**. We therefore measured the rate constants of the disproportionation and radical recycling reactions in addition to those of the DPPH• reaction. For the disproportionation the same solvents were used as for the DPPH• reaction, including ethanol, which was also used for the ubiquinol recycling, whereas a heterogeneous micellar system was chosen for the ascorbate recycling.

The primary reaction of the phenolic antioxidant with lipid peroxyl radicals (LOO•) will determine in part its biological efficiency, since it has to compete with the H-abstraction reaction of these radicals with polyunsaturated fatty acids, which was estimated to be rather slow ($k \approx 10$ L mol^{-1} s^{-1}).[62] In the case of successful detoxification of such radicals, the phenolic antioxidant is oxidized to a phenoxyl radical. Now essentially two pathways determine its fate. To recover the first antioxidant equivalent, the phenoxyl radical can undergo a redox reaction either with another phenoxyl molecule (disproportionation) or with a cellular reductant, such as

(58) Barclay, L. R. C.; Vinqvist, M. R. In *The chemistry of phenols*; Rappoport, Z., Ed.; John Wiley and Sons: Chichester, U.K., 2003; pp 839–908.
(59) Wang, X. Y.; Quinn, P. J. *Mol. Membr. Biol.* **2000**, *17*, 143–156.
(60) Hasford, J. J.; Rizzo, C. J. *J. Am. Chem. Soc.* **1998**, *120*, 2251–2255.
(61) Caffery, M. L.; Dobosh, P. A.; Richardson, D. M. *Laboratory Exercises using Hyperchem*; Hypercube, Inc.: Gainesville, FL, 1998.
(62) Buettner, G. R. *Arch. Biochem. Biophys.* **1993**, *300*, 535–543.

ascorbate and ubiquinol (reduced coenzyme Q). Disproportionation reactions have the disadvantage that one of two antioxidant molecules is lost in the form of a quinoid oxidation product. In contrast, the second pathway can recover both reducing equivalents and both antioxidant molecules. Therefore, the ratio of these two reactions determines the long-term efficiency of an antioxidant.[58] Furthermore, the formation of quinoid metabolites during disproportionation increases the risk of toxic side effects.[63] Although tocopheryl quinone (the quinoid oxidation product of **1**) in its reduced (quinol) state was considered a cellular antioxidant itself,[49] it is also known that many quinones can cause harm to the cell by ROS formation during redox cycling.[63]

The disproportionation rate constants ($2k_2$, Table 3) which reflect the radical stabilities, vary by more than 2 orders of magnitude in the group of compounds studied. The small $2k_2$ value, that is, high stability of the radical of **7**, is in line with its ESR spectrum (vide supra) and contrasts the relatively unstable radicals formed from **1**, **2**, **4**, and **6**, with **3** and **5** showing intermediate stability. That **3** forms a more stable radical than **1** was also evidenced from its ESR spectrum (vide supra). The rate constants for **1** and **2** in hexane are virtually identical with the values reported for the same compounds in benzene,[46] and the values in ethanol are similar to 1400 L mol^{-1} s^{-1} reported for **1** in the same solvent.[64] The large value for **4** may, at least in part, be attributed to the larger distortion of the aromatic plane compared to the other compounds, as seen from the calculated structure (see Experimental Section). Nevertheless this compound showed a slightly larger k_1 value than the trans isomer (**5**), suggesting that stereochemical factors play a role. Contrary to the primary antioxidant reaction (k_1), the disproportionation rates showed only small solvent effects and therefore should not depend on the exact location within biomembranes. For most compounds the rate constants are in good agreement with control values measured by ESR.

To maintain the antioxidative capacity of lipophilic phenolic antioxidants by avoiding their consumption as quinoid oxidation products, antioxidant recycling is important. A major pathway is considered to be the reduction of the phenoxyl radicals by hydrophilic coantioxidants such as ascorbate, which in turn can be recycled by glutathione.[58] This reaction seems to be essential for membranes or other lipophilic compartments such as LDL particles that have no enzymatic recycling systems for ubiquinol (vide infra). The rate constants (k_3, Table 4) determined for the phenoxyl reduction by ascorbate are in the range of 10^7−10^8 L mol^{-1} s^{-1} for the various antioxidants incorporated in cationic micelles (TTAB). This correlates well with the reported value of 7×10^7 L mol^{-1} s^{-1} for **1** incorporated in similar hexadecyltrimethylammonium chloride micelles.[16] This larger value for cationic micelles, compared to 4×10^4 L mol^{-1} s^{-1} for anionic SDS micelles[16] and 2×10^5 L mol^{-1} s^{-1} for zwitterionic phosphatidylcholine micelles[65] was explained on the basis of the ascorbate anion−micelle attraction. Our results show that ascorbate can recycle the novel chromanol-type antioxidants across the water−micelle interface, which is relevant to a possible pharmacological application.

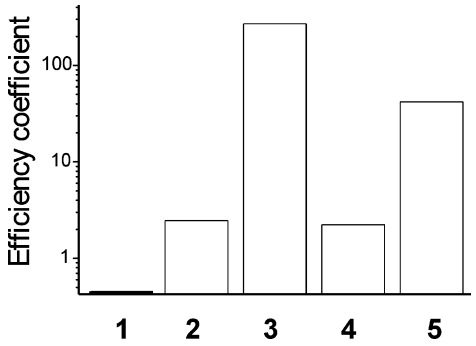

FIGURE 6. Overall antioxidant efficiency coefficient ($nk_1k_3k_4/2k_2$) of the novel antioxidants (**3**, **4**, and **5**) compared to **1** and **2**, where n is the stoichiometric factor, k_1 (Table 2) and $2k_2$ (Table 3) are expressed in liters per mole per second, k_3 (Table 4) in 10^7 liters per mole per second, and k_4 (Table 4) in 10^4 liters per mole per second. Rate constants obtained in ethanol were chosen for the calculation, except k_3, which was measured in an aqueous micellar system.

Whereas ubiquinol, an essential constituent of the mitochondrial inner membrane where it is continuously recycled, reacts 10 times more slowly with lipid peroxyl radicals compared to **1**,[58] it was suggested to be a major reductant for tocopheroxyl radicals.[20] The rate constants (k_4, Table 4) determined for the phenoxyl reduction by ubiquinol in ethanol are in the range 10^4−10^5 L mol^{-1} s^{-1}. The value for **1** is about 10 times smaller than the one measured by stopped-flow spectrometry in the same solvent.[21] Still, the results showed that in the presence of ascorbate or ubiquinol all antioxidants studied were recycled much faster than their disproportionation to ineffective (at least in terms of their antioxidant potency) quinoid products. In the case of **1** this explains the limited accumulation of α-tocopheryl quinone relative to α-tocopherol (1:20 to 1:100) observed in mitochondrial membranes.[66]

Conclusion

To evaluate the potential benefit of the new chromanols in the polar headgroup region of biomembranes, we define a formal overall antioxidant efficiency coefficient as ($nk_1k_3k_4/2k_2$) from results in ethanol/micellar systems, where n is the stoichiometric factor (number of reducing equivalents per molecule) and k_1−k_4 are the rate constants discussed above. This coefficient takes into account the various kinetic aspects associated with the antioxidant reaction of such compounds. Figure 6 shows these coefficients for those compounds for which all four rate constants could be measured (**3**, **4**, and **5**, and as a reference, **1** and **2**). It was evident that **3** showed by far the best overall antioxidant performance in these chemical model systems, even if the stoichiometric factor was set to unity for all compounds. Preliminary results on the subcellular level indicated that this may hold true

(63) Thornton, D. E.; Jones, K. H.; Jiang, Z.; Zhang, H.; Liu, G.; Cornwell, D. G. *Free Radical Biol. Med.* **1995**, *18*, 963−976.
(64) Rousseau-Richard, C.; Richard, C.; Martin, R. *FEBS Lett.* **1988**, *233*, 307−310.
(65) Scarpa, M.; Rigo, A.; Maiorino, M.; Ursini, F. *Biochim. Biophys. Acta* **1984**, *801*, 215−219.
(66) Gille, L.; Gregor, W.; Staniek, K.; Nohl, H. *Biochem. Pharmacol.* **2004**, *68*, 373−381.

also for the protection of respiratory functions of isolated mitochondria against oxidative damage (unpublished results). Taking together, the new compound twin-chromanol revealed the best set of kinetic parameters, its overall antioxidant efficiency exceeding that of α-tocopherol. This makes it a promising test candidate for further biological studies.

Experimental Section

Phenolic Antioxidants. *all-rac*-α-Tocopherol (**1**) and pentamethylchromanol (2,2,5,7,8-pentamethyl-1-benzopyran-6-ol; **2**) were obtained from commercial suppliers. The twin-chromanol (2,10-dihydroxy-6,12-methano-1,3,4,8,9,11-hexamethyl-12*H*-dibenzo[2,1-*d*:1′,2′-*g*]dioxocin; **3**) and oxachromanols (2,4,5,7,8-pentamethyl-4*H*-1,3-benzodioxin-6-ol; **4** and **5**) were synthesized according to Rosenau and co-workers.[23,24] Deuterated analogues of **4** and **5** (^{2,4}CD and ^{2a,4b}CD$_3$) were prepared from perdeuterated acetaldehyde.

Ubichromenol-9 (**7**; the index indicates the number of isoprene units) was synthesized by cyclization of 250 mg of ubiquinone-10 in 1 mL of deoxygenated triethylamine for 2 h at 95 °C according to Imada and Morimoto.[29] After removal of the solvent, the product was purified by column chromatography (Florisil), with a mixture of hexane/$CHCl_3$ (v/v = 8:2) as eluent. The UV spectrum (peaks at 275, 283, and 332 nm) of the slightly yellow fraction (ca. 20−45% yield) is identical to the published one.[25] ^{1}H NMR (300.13 MHz, $CDCl_3$): δ 1.38 (s, 3H, ^{2a}CH$_3$), 1.60 (s, 9 × 3H, $^{4'a,8'a,12'a,16'a,20'a,24'a,28'a,32'a,37'}CH_3$), 1.68 (s, 3H, *cis*-$^{36'a}CH_3$), 1.95−2.11 (m, 18 × prenyl CH$_2$), 2.16 (s, 3H, ^{5a}CH$_3$), 3.88 (s, 3H, OCH$_3$), 3.94 (s, 3H, OCH$_3$), 5.06−5.16 (m, 9H, prenyl CH), 5.42 (s, 1H, OH), 5.58 (d, 1H, ^3J = 10.1 Hz, ^{3}CH), 6.50 (d, 1H, ^3J = 10.1 Hz, ^{4}CH). ^{13}C NMR (75.47 MHz, $CDCl_3$): δ 10.3 (^{5a}C), 16.0 ($^{4'a,8'a,12'a,16'a,20'a,24'a,28'a,32'a}CH_3$), 17.7 (*cis*-$^{36'a}CH_3$), 22.8 ($^{2'}CH_2$), 25.5 (^{2a}CH$_3$), 25.7 (*trans*-$^{37'}CH_3$), 26.6−26.8 ($^{6',10',14',18',22',26',30',34'}CH_2$), 39.7 ($^{5',9',13',17',21',25',29',33'}CH_2$), 40.8 ($^{1'}CH_2$), 61.0 (OCH$_3$), 61.4 (OCH$_3$), 77.3 (^{2}C), 113.9 (^{5}C), 116.4 (^{4a}C), 119.8 (^{4}C), 123.9−124.7 ($^{3',7',11',15',19',23',27',31',35'}$CH), 129.0 (^{3}C), 131.2 ($^{36'}$C), 134.9−135.0 ($^{8',12',16',20',24',28',32'}$C), 135.4 ($^{4'}$C), 138.9 (^{6}C), 139.5 ($^{7,\ 8}$C), 140.4 (^{8a}C). The assignments were supported by H−H correlation spectroscopy (COSY), heteronuclear multiple quantum correlation (HMQC), and heteronuclear multiple bond correlation (HMBC) spectra. The absence of a carbonyl ^{13}C resonance (δ 185)[67] is indicative of the absence of UQ-10. The purity of **7** was determined by HPLC analysis to 95%.

Ubichromanol-9 (**6**), a cyclization product of ubiquinol, was obtained by selective reduction of **7** with sodium, analogous to a published procedure,[68] followed by column chromatography as for **7** (ca. 45−65% yield). Residual **7** was estimated by ^{1}H NMR to 3%. ^{1}H NMR (300.13 MHz, $CDCl_3$): δ 1.29 (s, 3H, ^{2a}CH$_3$), 1.60 (s, 9 × 3H, $^{4'a,8'a,12'a,16'a,20'a,24'a,28'a,32'a,37'}CH_3$), 1.68 (s, 3H, *cis*-$^{36'a}CH_3$), 1.79 (t, 2H, ^3J = 6.8 Hz, ^{3}CH$_2$), 1.95−2.11 (m, 18 × prenyl CH$_2$), 2.09 (s, 3H, ^{5a}CH$_3$), 2.57 (t, 2H, ^3J = 6.8 Hz, ^{4}CH$_2$), 3.85 (s, 3H, OCH$_3$), 3.93 (s, 3H, OCH$_3$), 5.06−5.16 (m, 9H, prenyl CH), 5.39 (s, 1H, OH). ^{13}C NMR (75.47 MHz, $CDCl_3$): δ 10.8 (^{5a}C), 16.0 ($^{4'a,8'a,12'a,16'a,20'a,24'a,28'a,32'a}CH_3$), 17.7 (*cis*-$^{36'a}CH_3$), 20.2 (^{4}C), 22.3 ($^{1'}CH_2$), 23.4 (^{2a}CH$_3$), 25.7 (*trans*-$^{37'}CH_3$), 26.6−26.8 ($^{2',6',10',14',18',22',26',30',34'}CH_2$), 31.1 (^{3}C), 39.7 ($^{5',9',13',17',21',25',29',33'}CH_2$), 60.8 (OCH$_3$), 61.3 (OCH$_3$), 75.1 (^{2}C), 116.0, 116.1 (^{4a,5}C), 124.1−124.4 ($^{3',7',11',15',19',23',27',31',35'}$CH), 131.2 ($^{36'}$C), 134.9−135.0 ($^{8',12',16',20',24',28',32'}$C), 135.3 ($^{4'}$C), 138.2 (^{6}C), 139.1, 139.6, 140.5 ($^{7,\ 8,8a}$C). The assignments were supported by H−H COSY, HMQC, and HMBC spectra.

Other Chemicals. Chromatography-grade acetonitrile (LiChrosolv; $H_2O \leq 0.05\%$) and ethanol (LiChrosolv; $H_2O \leq 0.1\%$) as well as spectroscopy-grade *n*-hexane (Uvasol; $H_2O \leq 0.005\%$) were used. Decylubiquinol ($dUQH_2$) was prepared by reduction of dUQ with sodium dithionite in water/ethanol (1:1) followed by hexane extraction.[12]

Electron Spin Resonance Spectra of Phenoxyl Radicals. Compounds **1**−**5** (50 mM each) were dissolved in benzene or benzene/acetonitrile (v/v = 10:1). Oxygen was removed by flushing with nitrogen. The samples were transferred to a 0.9 × 5.5 cm quartz flat cell and irradiated with a high-pressure Hg UV lamp inside the TM cavity of a Bruker ESP 300 X-band spectrometer. Instrumental settings: microwave frequency, 9.76 GHz; microwave power, 20 mW; receiver gain, 10^6; modulation frequency, 100 kHz; modulation amplitude, 0.25 G (**1**, **4**, **5**) or 0.1 G (**2**, **3**); scan rate, 17.9 G/min; time constant, 167 ms; temperature, 298 K; 6 scans per spectrum were averaged.

ESR spectra of the radicals of **6** and **7** were measured with a Bruker EMX X-band spectrometer equipped with a TE cavity. The radicals were generated by briefly stirring a 3 mM solution of the antioxidant in argon-deaerated benzene in a 3 mm (i.d.) ESR quartz tube containing a few grains of PbO_2. Instrumental settings: microwave frequency, 9.77 GHz; microwave power, 20 mW; receiver gain, 10^6; modulation frequency, 100 kHz; modulation amplitude, 0.05 G; scan rate, 22 G/min; time constant, 82 ms; temperature, 298 K; 20 scans were averaged.

Using the results of the quantum chemical calculation (vide infra) as starting parameters, analysis of the hyperfine splitting structure was done by two different iterative ESR simulation programs (ESRSIMU of our own design and WINSIM[69]) until the sum of error squares reached a minimum. Both programs yielded essentially the same coupling constants.

Quantum Chemical Prediction of Hyperfine Coupling Constants for Phenoxyl Radicals. The structures of the phenoxyl radicals were assembled in the molecular modeling program HyperChem[31] and the geometries were preoptimized on the semiempirical level (PM3/UHF). These structures were imported into the program Gaussian98[38] and the structures were reoptimized on the DFT level [B3LYP/6-31G(d)].[37] From the output file, the Fermi contact coupling constants were obtained. For freely rotating methyl and methoxy groups, the three coupling constants of the H-atoms were averaged to give one isotropic coupling constant. To keep computation times reasonably short, the short-chain analogues **2**, ubichromanol-1, and ubichromenol-1 were calculated for the radicals derived from **1**, **6**, and **7**, respectively.

Optical Spectra of Phenoxyl Radicals. UV/Vis spectra of the radicals were measured on a Spectronic 3000 diode-array spectrophotometer (Milton Roy; slit width 1.75 nm). The radicals were generated either photolytically by a 2-min (**1**, **2**, and **4**) or 5-min (**3** and **5**) irradiation (generating saturating steady-state concentrations) of 50 mM aerobic solutions of the chromanols in acetonitrile, by use of a focused high-pressure Hg UV lamp and a cuvette holder kept at 20 °C, or by reaction of 1 mM chromanol with 20 μM (final concentration) of the stable radical diphenyl picryl hydrazyl (DPPH$^\bullet$), both in acetonitrile. Alternatively, the radicals were generated with PbO_2 as described below. Since the spectra of irradiated **6** and **7** were dominated by oxidation/decay products other than the expected radicals, these were generated exclusively by the DPPH$^\bullet$ reaction. Baseline scans of the antioxidants prior to radical formation were subtracted.

Stopped-Flow Photometry of the DPPH$^\bullet$ Reaction. The kinetics of the antioxidant reaction with DPPH$^\bullet$ as well as the decay of the resulting phenoxyl radical were measured on a DW2000 dual-wavelength spectrophotometer (SLM Aminco) equipped with a dual-channel MilliFlow stopped-flow reactor (kept at 20 °C) by the same manufacturer. Acetonitrile, ethanol, and *n*-hexane were used as solvents. For comparison, argon-deaerated or freshly distilled solvents were used. Defined concentrations of **6** and **7** (2−7 mM, determined from

(67) Boullais, C.; Rannou, C.; Reveillere, E.; Mioskowski, C. *Eur. J. Org. Chem.* **2000**, *5*, 723−727.
(68) Schudel, P.; Mayer, H.; Metzger, J.; Rüegg, R.; Isler, O. *Helv. Chim. Acta* **1963**, *46*, 2517−2526.
(69) Duling, D. R. *J. Magn. Reson. B* **1994**, *104*, 105−110.

OD_{293} and OD_{332} by use of $\epsilon = 3480$ and 3230 L mol^{-1} cm^{-1} in ethanol, respectively[25]) or 8 mM for all other chromanols were mixed with 200 μM DPPH$^\bullet$ except for **3** in hexane: because of its low solubility, 120 μM (determined from OD_{290} by use of $\epsilon = 5900$ L mol^{-1} cm^{-1} in ethanol) was mixed with 6 μM DPPH$^\bullet$. The decay of DPPH$^\bullet$ (eq 2) was followed at 520 nm (acetonitrile), 517 nm (ethanol), or 511 nm (hexane). The transient formation and subsequent decay of the phenoxyl radicals were followed at the peak of their absorption around 420 nm (except 475 nm for **7**; see Table 1). A reference wavelength of 850 nm was chosen at which the absorptions of both DPPH• and its reduced product were negligible.

The traces of the DPPH$^\bullet$ decay were set to zero at infinite time. Since antioxidants were in large excess over DPPH$^\bullet$, these plots were fitted (by the nonlinear least-squares method of Levenberg−Marquardt) to pseudo-first-order decay:

$$A = A_0 \exp(-ak_1 t) \tag{12}$$

where A_0 is the DPPH$^\bullet$ absorption at time zero, k_1 is the second-order rate constant for the reaction of the antioxidant with DPPH$^\bullet$, and a is the excess antioxidant concentration. A_0 and k_1 were kept variable. Since a similar zeroing of the slowly decaying tail of the phenoxyl decay (eq 3) would be error-prone, the absorption plots were fitted to

$$A = A_{\text{offset}} + \frac{A_0 - A_{\text{offset}}}{1 + (A_0 - A_{\text{offset}})\, 2k_2\epsilon^{-1}t} \tag{13}$$

where A_0 is the absorption at time zero, A_{offset} is the absorption offset, $2k_2$ is the second-order rate constant for the disproportionation, and ϵ is the molar extinction coefficient of the phenoxyl radical as determined (vide infra). Only part of each plot representing the pure decay, starting at the time of complete DPPH$^\bullet$ consumption (as determined from the respective DPPH$^\bullet$ plots), was fitted. Good fits were obtained by choosing A_0, A_{offset}, and k_2 as variables.

ESR Measurements of the Phenoxyl Radical Decay. Antioxidant (50 mM, except 4 mM **6** and 1.5 mM **7**) was mixed (within ca. 5 s) with 20 mM (except 2 mM for **6** and 0.6 mM for **7**) DPPH$^\bullet$, both in acetonitrile, with reduced pressure into a flat cell equipped with a rubber plunger carrying two needles. At these concentrations the DPPH$^\bullet$ decay was complete after 5 s (20 s for **6**, 80 s for **7**), in agreement with the rate constants determined from stopped-flow analysis (vide supra). At 15−20 s (30 s for **6**, 90 s for **7**) after mixing, repetitive ESR spectra were measured. Instrumental settings: microwave frequency, 9.67 GHz; modulation amplitude, 0.5 G; scan rate, 21 G/min; repetition time, 25 s; others as above. The peak-to-peak intensities of the largest peak (the sum of the three largest peaks for the noisier spectra from **4**) were converted to radical concentrations by calibration with 200 μM DPPH$^\bullet$ in acetonitrile, which was measured after each sample, by use of the same instrumental settings without retuning. The decay plots were fitted to

$$c = \frac{c_0}{1 + (c_0 2k_2 t)} \tag{14}$$

where c_0 is the phenoxyl concentration at time zero and $2k_2$ is the second-order rate constant for the disproportionation (eq 3).

Other Measurements of the Phenoxyl Radical Decay. The phenoxyl radicals were also generated by briefly vortexing a 1 mM antioxidant solution (except 10 mM **6** and **7**) in acetonitrile with ca. 1 mg of PbO_2. After a brief centrifugation at 15000*g*, the supernatant was quickly transferred to a cuvette, and time scans were measured at the peak of their absorption around 420 nm (see Table 1) and at 850 nm (as reference) on a diode-array photometer (vide supra). The 420 minus 850 difference traces were analyzed by use of eq 13.

Laser Flash Photolysis and Antioxidant Recycling. The rate constants (k_3) of the chromanoxyl reduction by ascorbate (eq 4) were measured by laser photolysis of the antioxidants incorporated in aqueous cationic micelles. Compound **6** or **7** (100 μL) in *tert*-butyl alcohol was evaporated to dryness in a glass vial and resuspended in a 40 °C warm solution of 200 mM TTAB and 25 mM potassium phosphate (pH 6.8) by 5 min of vortexing, to give a final antioxidant concentration of 1 mM. Similarly, 200 mM solutions of all other antioxidants (except a 50 mM suspension of **3**) in methanol were added to 40 °C warm 40 mM TTAB micelles in the same buffer under vortexing, and vortexing was continued for 5 min. Radical concentrations of ca. 1−10 μM were generated by flashing these micellar solutions, preloaded with ascorbate, with a series (10−30) of 10 ns, 266 nm pulses from a Nd:YAG laser (Quanta-Ray DCR-1) at a repetition rate of ca. 1 Hz at room temperature. Details of the experimental setup have been published previously.[70] For each compound, three different ascorbate concentrations (0.2, 0.4, and 0.6 mM) and three different pulse energies (ca. 0.4−1 mJ) were applied. The radical decay was monitored photometrically at the peak of the respective radical spectrum around 420 nm.

The rate constants (k_4) of the chromanoxyl reduction by ubiquinol (eq 8) were measured similarly in ethanolic solution. Compounds **1**, **2**, **4**, and **5** (100 mM), **3** (10 mM; saturated solution), and **6** and **7** (4 mM) were used. The laser was tuned to 355 nm, and 10 mM azo initiator AMVN was added to the reaction mixture. For each compound, three different decylubiquinol concentrations (1, 2, and 4 mM except 4, 8, and 12 mM for **1**) were chosen; the pulse energy was in the 0.5−2 mJ range.

The traces were analyzed by a pseudo-first-order fit, taking into account a simultaneous second-order decay of the radical with a rate constant ($2k_2$) measured in the absence of reductant, by use of eq 17. It should be noted that this second-order reaction was faster than the disproportionation reaction as measured by stopped-flow, presumably because of the presence of additional photogenerated radicals. However, under our conditions the half-life of this reaction was considerably longer than that of the reaction with the reductant.

$$\text{PhO}^\bullet + \text{reductant} + \text{H}^+ \xrightarrow{k_{\text{red}}} \text{PhOH} + \text{oxidized reductant} \tag{15}$$

$$2\ \text{PhO}^\bullet \xrightarrow{k_2} \text{products} \tag{16}$$

$$A = A_{\text{offset}} + \frac{k_{\text{pseudo}} A_0}{(k_{\text{pseudo}} + A_0 2k_2)\exp(k_{\text{pseudo}}\, t) - A_0 2k_2} \tag{17}$$

where A_{offset} is the absorption offset (accounting for possible minor side reactions), A_0 is the phenoxyl absorption at time zero, $2k_2$ is the rate constant of the second-order decay, and $k_{\text{pseudo}} = c_{\text{red}} k_{\text{red}}$ with c_{red} the excess reductant concentration and k_{red} the second-order rate constant for the reaction of phenoxyl with ascorbate (k_3) or ubiquinol (k_4). A_0, A_{offset}, and k_{pseudo} were kept variable. Comparable results were obtained with the numerical simulation routine used for the stopped-flow experiments (vide supra).

In the case of **7** the expected chromenoxyl radical could not be detected. Therefore a lower limit of the rate constants was estimated by oxidizing 1 mM **7** in micellar solution or 4 mM **7** in ethanol with ca. 1 mg of PbO_2 (by vortexing for 1 min or a few seconds, respectively), transferring the supernatant to a cuvette after a brief centrifugation, admixing ascorbate or decylubiquinol, respectively, from a premounted syringe under magnetic stirring, and monitoring the radical decay at 475

(70) Baranyai, P.; Gangl, S.; Grabner, G.; Knapp, M.; Köhler, G.; Vidóczy, T. *Langmuir* **1999**, *15*, 7577−7584.

minus 850 nm with a DW2000 photometer (SLM Aminco) on the fast filter setting.

Stoichiometry of Antioxidant Reaction. Antioxidant (10 μM) in freshly distilled acetonitrile was oxidized with 60 μM DPPH$^\bullet$ (final concentration) after addition of 0−50% H_2O, and the reaction was monitored in a DW2000 photometer (SLM Aminco) at 520 nm minus 850 nm until the DPPH$^\bullet$ concentration was constant. From the extent of DPPH$^\bullet$ reduction, the number of reducing equivalents of the antioxidants was calculated, by use of an extinction coefficient of 11 600 L mol^{-1} cm^{-1} (determined relative to 11 200 L mol^{-1} cm^{-1} in ethanol).[71]

Calculation and Measurement of Octanol/Water Distribution Coefficient. Experimental log *P* values were calculated from the antioxidant absorptions (around 290 nm) in the organic and water phases after equilibration of 1 mL of 500 mM **1** and **2**, 100 mM **4** and **5**, 30 mM **3**, 50 mM **6**, or 10 mM **7** in *n*-octanol with 1 mL water by vortexing under argon for 25 min (**1**), 45 min (**6** and **7**), or 15 min (others) at 20°C. Longer vortexing had no effect on log *P*. Prediction of log *P* values was performed by an incremental method[32,33] that was used by the QSAR module of HyperChem.

Measurement of Extinction Coefficients of Phenoxyl Radicals. Antioxidant (100 mM, except 80 mM **3** and 5 mM **6** and **7**) in acetonitrile or ethanol was loaded into a cuvette kept at 5 °C (to minimize evaporation loss, except **6**, which was kept at 20 °C) and a baseline scan was recorded on a diode-array photometer (vide supra). After admixing of 10 μM DPPH$^\bullet$ (except 20 μM for **3**; final concentrations) in the same solvent within 5 s, 4−5 spectra of the resulting radicals were measured with a repetition time of 5 s (3 nm slit width). After a linear baseline was subtracted from each scan (to account for baseline drifts), peak intensities were plotted against time and extrapolated to time zero via a nonlinear fit for the bimolecular radical decay (eq 14). At the chosen concentrations, the radicals reached their maximal concentration after ca. 1−5 s and subsequently decayed almost linearly, as predicted from the measured rate constants k_1 and k_2 (vide supra), minimizing extrapolation errors. The molar extinction coefficients (ϵ) were calculated from the extrapolated absorptions.

Semiempirical Quantum Chemistry Methods. Structures of the phenolic antioxidants were assembled in the program HyperChem[31] and subjected to a geometry optimization by the semiempirical method PM3/UHF, yielding HOMO and LUMO energies. Again the short-chain analogues **2**, ubichromanol-1, and ubichromenol-1 were calculated for **1**, **6**, and **7**. The O−H bond dissociation enthalpies (BDE) were obtained from the calculated enthalpies of formation of PhOH, PhO$^\bullet$, and H$^\bullet$ by use of PM3/UHF optimized structures.

Abbreviations

AMVN, 2,2′-azobis(2,4-dimethylvaleronitrile); asc, ascorbate; BDE, bond dissociation enthalpy; DPPH$^\bullet$, diphenyl picryl hydrazyl; $dUQH_2$, decylubiquinol; ESR, electron spin resonance; HOMO, highest occupied molecular orbital; LUMO, lowest unoccupied molecular orbital; PhOH, phenolic antioxidant; PhO$^\bullet$, phenoxyl (chromanoxyl) radical; PhQ, quinoid oxidation product; ROS, reactive oxygen species; TTAB, tetradecyl trimethylammoniumbromide; UQ, ubiquinone.

Acknowledgment. This work was supported by the Austrian Science Fund (FWF), Grant P16244-B08. Technical assistance by Werner Stamberg and helpful advice for the synthesis of **6** by Dr. Thomas Netscher (DSM Nutritional Products, Basel, Switzerland) is gratefully acknowledged.

Supporting Information Available: Cartesian coordinates and total energies of the calculated molecular structures of chromanoxyl radicals (PDF). This material is available free of charge via the Internet at http://pubs.acs.org.

JO047927S

(71) Tampo, Y.; Yonaha, M. *Arch. Biochem. Biophys* **1996**, *334*, 163−174.